

# Obstacle Avoidance for a Quadrotor

Nikoli Dryden \*

Bryan Plummer †

## Abstract

We implement and evaluate the approach of [Lee et al. 2011] for obstacle avoidance for an ARDrone 2 quadrotor, which integrates MOPS and SIFT features to get a sparse representation of obstacles. We also evaluate the existing PTAM [Klein and Murray 2007] approach to UAV navigation. We find that the MOPS features are not robust on the quadrotor's data and that the Lee et al. approach is both ineffective and computationally intensive whereas the PTAM system achieves robust, real-time performance.

## 1 Introduction

Micro aerial vehicles(MAV's), which include quadrotor and unmanned aerial vehicles(UAV's), have the potential to become more prominent over the next several years. These aircraft allow easy access for many places which are difficult for humans to go in a safer manner for both humans and the environment and have applications reaching into search and rescue, tracking, mapping, and others. In order for the higher level tasks to be handled these vehicles must have a reliable navigation system.

There are GPS solutions for navigation work out of the box (e.g. the AscTec series of quadrotors), but are limited in use to locations where GPS is available. While much progress has been made to solve to create a navigation solution for these cases, we still strive to have a system that works in unknown, GPS denied, and cluttered environments. As many MAV's are limited in both carrying capacity and power, laser range finders are too heavy and consume too much power to be of use. Stereo camera's become highly inaccurate after a set distance rendering them of no more use than using a single camera.

The common structure from motion approach to visual navigation using a single camera has been shown to suffer from some drawbacks. In order to generate a 3D map, two types of camera translation may be necessary [Shah et al. 2010]. While a quadrotor may be capable of such a maneuver, a UAV is not. In [Shah and Johnson 2009] the amount of computation required using this approach increased by about 15 times with only an increase from 8 to 35 feature points, and the number of features in a real scene can number in the hundreds or thousands.

As an attempt to solve this problem [Lee et al. 2011] proposed an approach to reduce the number of points required to represent the 3D structure of a scene. The authors used multiscale oriented patches(MOPS) [Brown et al. 2005] to create outlines of objects. Since the outlines themselves are unable to tell if an outline is empty or not, they used the 3D location of SIFT features [Lowe 2004] located within the outlines to obtain this information.

Although the proposed method cited collision avoidance for a quadrotor as its intended application, the authors did not dispense any data on its effectiveness in real scenes from images taken using a quadrotor. This paper provides just such an evaluation using images taken from the AR-Drone 2.0 quadrotor with the processing being performed on a laptop obtaining the images from the quadrotor through a wireless network. In addition, we evaluate the use of the parallel tracking and mapping(PTAM) [Klein and Murray

2007] approach that was adapted as an online solution for quadrotors in [Weiss et al. 2011].

## 2 Related Work

Due to weight and energy restrictions aboard MAV's a vision based approach is seen as one of the most viable navigation solutions in GPS denied environments. Progress in using visual sensors for navigation purposes include performing specific tasks such as in [Johnson et al. 2005] where a single camera was used to guide and land a MAV, or [Huang et al. 2011] where an RGB-D camera was used to map an environment and localize a quadrotor within that map but is restricted for use in indoor environments.

Another common approach in the literature uses optical flow to estimate the relative motion between the frames of a camera. In these systems one is able to detect collisions by measuring the relative rate of expansion of objects. This method behaves poorly when light intensity doesn't remain constant [Horn and Schunck 1981] and tends to be sensitive to noise and an unstable camera. As all MAV's will contribute to some vibrations in the camera this leads to inaccurate estimates in flow vectors.

Some recent work attempts to use image segmentation to identify an obstacle and build a dense map around it [Ha and Sattigeri 2012]. This approach shares some motivations as the first method attempted in this work in that it attempts to reduce the number of computations required for navigation by using a limited number of feature points. As with [Lee et al. 2011], this approach has only been evaluated on theoretical data. The authors note that in some cases image segmentation is not possible and intend to evaluate and extend their work to ascertain the extent this kind of information is beneficial to navigation.

## 3 Approach

We begin by describing our implementation of the approach in [Lee et al. 2011]. Subsequently, we introduce a variation we attempted to generate an improved 3D map than we obtained using the unmodified version of [Lee et al. 2011]. Lastly, we describe our integration of the PTAM system with the quadrotor.

### 3.1 Lee et al.'s Method

Our approach closely follows that in [Lee et al. 2011]. The goal is to make use of MOPS features to limit the number of SIFT features necessary for computing structural information about obstacles. We begin by assuming that we have, as input, two images taken from the quadrotor's forward-facing camera, that the images are of the same scene, and contain corresponding features. For our purposes, we need only a greyscale image and so discard the colour information.

In each image, we compute MOPS descriptors [Brown et al. 2005]. The descriptors are located at features detected by a multi-scale Harris corner detector. Each descriptor is an  $8 \times 8$  patch of bias/gain normalized intensity values and is oriented using a blurred local gradient. Feature density is controlled using an adaptive non-maximal suppression algorithm. SIFT descriptors [Lowe 2004] are also computed, using the OpenCV computer vision library \*\*\* CITE OpenCV \*\*\*.

\*dryden2@illinois.edu

†bplumme2@illinois.edu

Descriptors in these two images are then matched in order to generate putative matches. For MOPS, matching is performed using a brute-force matcher, since existing  $k$ -d tree implementations in OpenCV do not support efficient dynamic modification after creation. SIFT features are matched using OpenCV's FLANN fast approximate nearest-neighbour [Muja and Lowe 2009] matcher.

These matches are then used to determine the location of the detected feature points in three-dimensional space via triangulation. Our approach to triangulation is based on the one implemented in PTAM \*\*\* CITE PTAM code \*\*\*. A homography is first computed between matching points. This homography is then decomposed into rotation and translation matrices [Malis and Vargas 2007] which are used to determine a projection matrix. This is used to triangulate points as usual.

In our implementation, the above steps involving SIFT and MOPS are implemented in parallel using the standard pthreads \*\*\* CITE pthreads? \*\*\* library. Since to this point there are no interactions between the SIFT and MOPS features and the input images are constant, the operations are independent. We thus run each in a separate thread in order to maximize performance.

The locations of MOPS features indicate the corners of objects in the world. The orientation of the descriptors is used to extract the outlines of objects to obtain edge spatial information. However, this does not provide information on the internal structure of the object; we use the SIFT features to achieve this. We consider SIFT features within the outlines constructed by MOPS features, which provide information on the internal structure of the objects: the distance to the points will indicate the type and extent of the object. An example of merged SIFT and MOPS features from [Lee et al. 2011] is provided in Figure 1.

We now determine the “type” of the object, based on comparison of the distance of SIFT features within an outline to the distance to MOPS features on the outline. Define  $D_M$  to be the distance to a MOPS feature, and  $D_S$  to be the distance to a SIFT feature within the outline. Let  $T_1$  and  $T_2$  be two threshold values. We have the following equations

$$|D_M - D_S| \leq T_1 \quad (1)$$

$$T_1 < |D_M - D_S| \leq T_2 \quad (2)$$

$$T_2 < |D_M - D_S| \quad (3)$$

$T_1$  should be set such that there is a high probability that the SIFT and MOPS features are on the same object, and  $T_2$  such that there is a high probability that the features are on different objects. We thus have the following cases:

- Equation 1 is the case of an object with a closed interior.
- Equation 2 is again the case where an object has a closed interior, but possibly with a convex shape.
- Equation 3 is the case of an object with an open interior.

In the third case, we repeat the above process feature points on an object behind the open space.

This comparison allows us to determine what sort of obstacle an object is and to locate where in the world the objects exist, relative to the quadrotor.

## 3.2 Replacing MOPS with Contours

After finding object outlines using MOPS features to not give an insufficient amount of information, we sought an alternative approach. As [Suzuki and Abe 1985] has been widely tested and locates contours within an image it appeared to be sufficient to meet

our needs. We used the Canny Edge Detector [Canny 1986] to convert to binary images as the input to this method. After locating the contours in an image we marked the key points found using the SIFT algorithm as belonging to an object outline and proceeded as normal through the rest of the approach of [Lee et al. 2011] as normal.

## 3.3 Integrating PTAM

Integrating PTAM with the quadrotor is remarkably simple. We made use of two different methods to accomplish this, in order to have different features available. Both methods rely upon the Robot Operating System (ROS) \*\*\* CITE ROS \*\*\* for support and the ardrone\_autonomy \*\*\* CITE ardrone\_autonomy \*\*\* driver for communication with the quadrotor.

Our first approach is to directly test PTAM on data from the quadrotor. For this, we made use of the ethzasl\_ptam package \*\*\* CITE ethzasl\_ptam \*\*\* which integrates PTAM with ROS. It was then only a matter of converting the camera stream from the ardrone\_autonomy driver to the requisite format for use with PTAM and calibrating the camera appropriately.

Secondly, we made use of the tum\_ardrone \*\*\* CITE tum\_ardrone \*\*\* package for ROS, which integrates a version of PTAM with an extended Kalman filter for data fusion and state estimation and a system for generating steering commands for the quadrotor. tum\_ardrone builds upon PTAM to provide an environment specifically designed for use with the ARDrone and ARDrone 2, and in addition to obstacle detection, provides a system for navigation and auto-pilot.

## 4 Experiments

Our data sets consist of samples obtained by recording output from the quadrotor's forward-facing camera. These are  $640 \times 360$  pixel colour images saved in JPEG format recorded at a rate of one per each 0.01 second. Our initial data sets consisted of

- A set of 212 frames in which the drone is sitting still on a table.
- A set of 321 frames in which the drone takes off, flies down a Siebel Center hall, and lands.
- A set of 301 frames in which the drone takes off, flies through the Siebel Center atrium, and lands.

These were supplemented with the following additional data sets from the quadrotor, this time recorded at a rate of one per each 0.1 second.

- A set of 130 frames in which the drone flies through the Siebel Center atrium with additional movement, and people present.
- A set of 275 frames in which the drone flies closely along the pillars and display cases of in the Siebel Center atrium.
- A set of 49 frames in which the drone flies towards a corner in the Siebel Center atrium.



**Figure 1:** Example output for combined SIFT and MOPS features.

#### 4.1 Lee et al.

#### 4.2 PTAM

### 5 Analysis

### 6 Individual Contributions

Individual contributions break down roughly as follows. Nikoli was responsible for:

- Implementing SIFT feature detection, extraction, and image matching
- Implementing 3-D reconstruction and triangulation
- Implementing the multi-threaded image pipeline
- Setting up and integrating ethzasl\_ptam with the quadrotor
- Setting up tum\_ardrone
- Experimental evaluations
- Presentation and paper writing

Bryan was responsible for:

- Implementing MOPS feature detection, extraction, and image matching
- Experimenting with a contour-based technique to replace MOPS
- Assistance with 3-D reconstruction
- Assistance with setting up ethzasl\_ptam
- Experimental evaluations

- Presentation and paper writing

Because MOPS was implemented from scratch, we feel that the work was split quite evenly.

### References

- BROWN, M., SZELISKI, R., AND WINDER, S. 2005. Multi-image matching using multi-scale oriented patches. In *CVPR*.
- CANNY, J. 1986. Computational approach to edge detection. *PAMI* 8, 6, 679–698.
- HA, J., AND SATTIGERI, R. 2012. Vision-based obstacle avoidance based on monocular SLAM and image segmentation for UAVs. In *Proc. AIAA Infotech@Aerospace Conference*.
- HORN, B., AND SCHUNCK, B. 1981. Determining optical flow. *Artificial Intelligence* 17, 1–3, 185–203.
- HUANG, A. S., BACHRACH, A., HENRY, P., KRAININ, M., MATURANA, D., FOX, D., AND ROY, N. 2011. Visual odometry and mapping for autonomous flight using an RGB-D camera. In *Int. Symposium on Robotics Research (ISRR)*.
- JOHNSON, A., MONTGOMERY, J., AND MATTHIES, L. 2005. Vision guided landing of an autonomous helicopter in hazardous terrain. In *IEEE International Conference on Robotics and Automation*.
- KLEIN, G., AND MURRAY, D. 2007. Parallel tracking and mapping for small AR workspaces. In *Proc. Sixth IEEE and ACM International Symposium on Mixed and Augmented Reality (ISMAR'07)*.
- LEE, J., LEE, K., PARK, S., IM, S., AND PARK, J. 2011. Obstacle avoidance for small UAVs using monocular vision. *Aircraft Engineering and Aerospace Technology* 83, 6, 397–406.

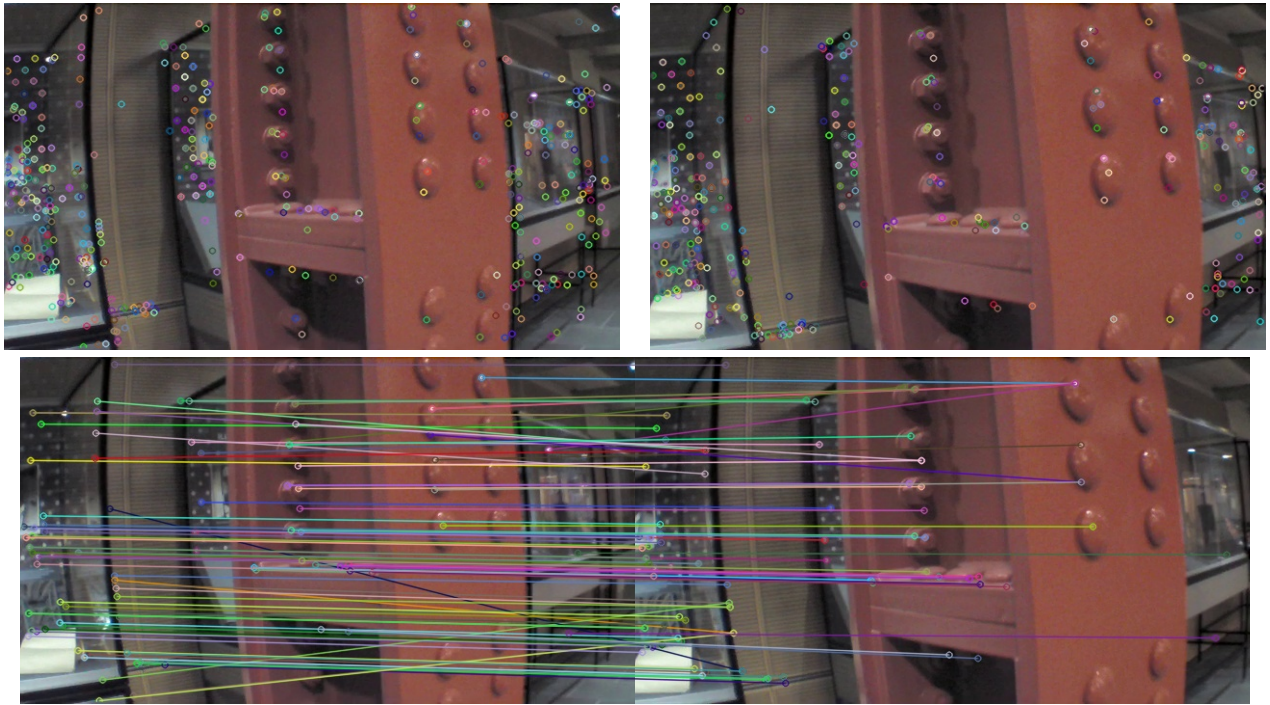


**Figure 2:** *SIFT keypoints and matches.*

- LOWE, D. G. 2004. Distinctive image features from scale-invariant keypoints. *IJCV* 60, 2, 91–110.
- MALIS, E., AND VARGAS, M. 2007. Deeper understanding of the homography decomposition for vision-based control. Tech. rep.
- MUJA, M., AND LOWE, D. G. 2009. Fast approximate nearest neighbors with automatic algorithm configuration. In *International Conference on Computer Vision Theory and Application VISSAPP'09*, INSTICC Press, 331–340.
- SHAH, S. I. A., AND JOHNSON, E. N. 2009. 3D obstacle detection using a single camera. In *Proc. AIAA Guidance, Navigation, and Control Conference*.
- SHAH, S. I. A., KANNAN, S., AND JOHNSON, E. N. 2010. Motion estimation for obstacle detection and avoidance using a single camera for UAVs/robots. In *Proc. AIAA Guidance, Navigation, and Control Conference*.
- SUZUKI, S., AND ABE, K. 1985. Topological structural analysis of digitized binary images by border following. 32–46.
- WEISS, S., SCARAMUZZA, D., AND SIEGWART, R. 2011. Monocular-SLAM-based navigation for autonomous micro helicopters in GPS-denied environments. *Journal of Field Robotics* 28, 6, 854–874.



**Figure 3:** *MOPS keypoints and matches.*



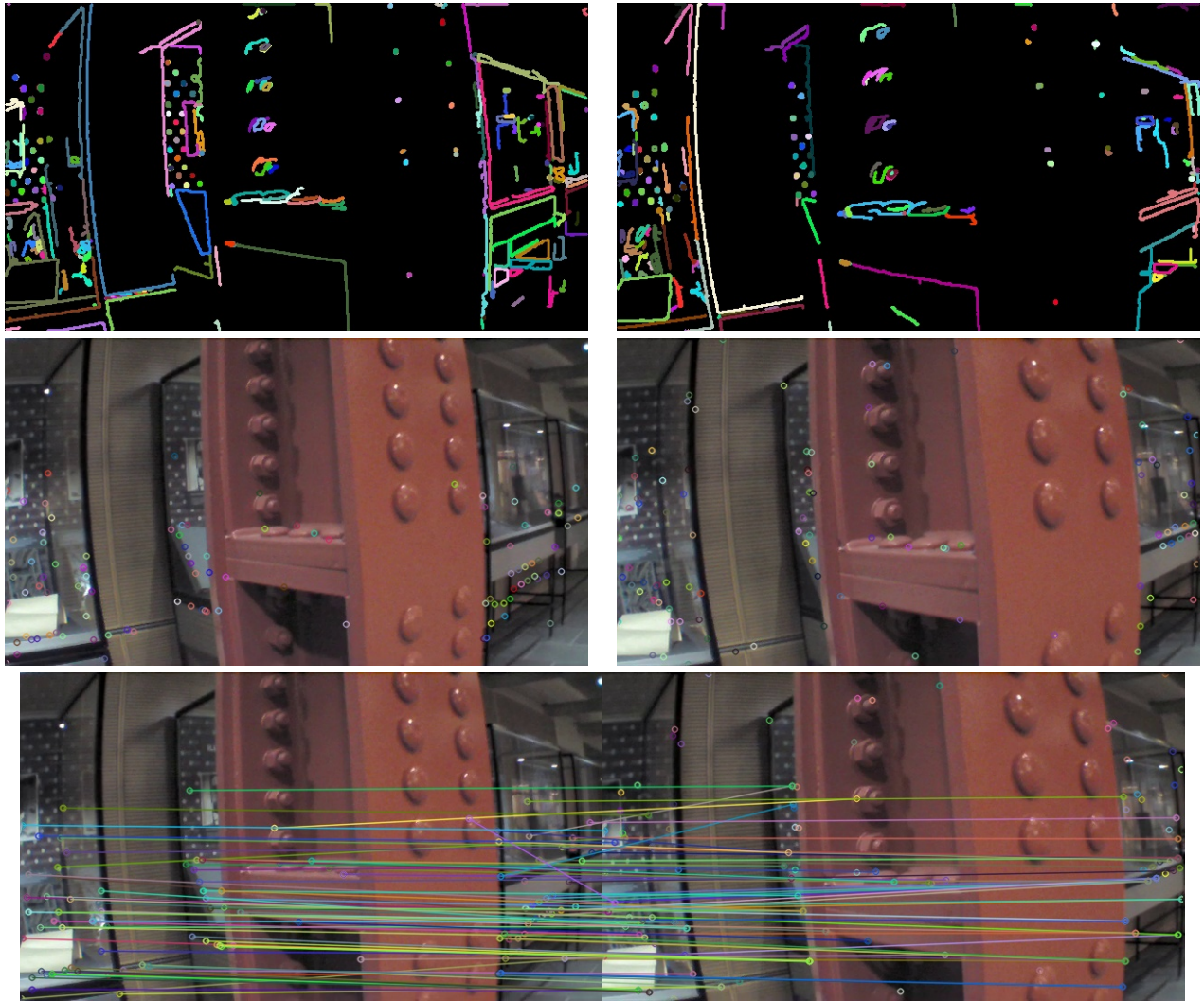


**Figure 4:** *Contour lines, keypoints, and matches.*

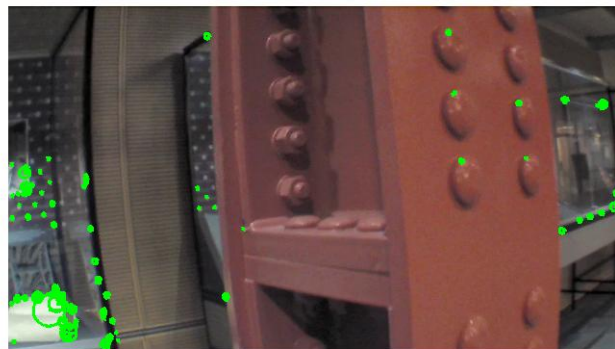


**Figure 5:** *VLFeat multi-scale Harris corner detector keypoints.*